INTERNATIONAL JOURNAL FOR NUMERICAL METHODS IN FLUIDS, VOL. 20, 493–506 (1995)

EFFICIENT MOULD FILLING SIMULATION IN CASTINGS BY AN EXPLICIT FINITE ELEMENT METHOD

R. W. LEWIS, A. S. USMANI AND J. T. CROSS

Institute for Numerical Methods in Engineering, University College of Swansea, Swansea, SA2 8PP, U.K.

SUMMARY

A model for simulating the process of mould filling in castings is presented. Many defects in a casting have their origins at the filling stage. Numerical simulation of this process can be of immense practical benefit to the foundry industry, however a rigorous analysis of this process must model a wide range of complex physical phenomena. In order to contain the costs and complexity that would be necessary for such a model, certain simplifying assumptions have been made. These assumptions limit the scope of this model to only predicting realistic thermal fields during the filling process.

A laminar regime has been assumed for the flow field, which is obtained by solving the incompressible Navier–Stokes equations using a velocity–pressure segregated semi-implicit finite element method. The free metal surface is predicted by advecting a pseudo-concentration function via the computed flow field. This involves an explicit finite element solution of a pure advection equation. The thermal field is calculated by solving the convective–diffusive energy equation by an explicit finite element method using the computed flow field and the location of the free surface. All the advection terms are discretized using a Taylor–Galerkin method. The interface between the metal and mould is modelled using special interface elements.

The model is demonstrated by solving practical example problems. The results show that a sharp thermal front is maintained during the course of filling without excessive diffusion. The heat diffusion in the mould can be controlled by varying the metal mould heat transfer coefficient.

KEY WORDS: finite element method; mould filling; explicit Taylor–Galerkin; pseudo-concentration; interface elements

INTRODUCTION

The numerical prediction of realistic flow patterns in the filling of a metal casting is an extremely difficult task. With *state of the art* numerical methods for incompressible flow, it is doubtful that realistic flow simulations in castings can ever be achieved regardless of the cost. However, some form of filling and thermal analysis is essential for a reliable prediction of the cooling and solidification of castings, coupled with residual stress and distortion calculations. This is because the accuracy of a heat transfer and stress analysis of a casting is partly dependent upon the knowledge of the true initial conditions. As these are the conditions at the end of the filling process, a good filling analysis should provide a reasonable approximation. If the filling time obtained from the flow analysis of a casting is close to reality, one may reasonably use the values of the temperature and the velocity field at the end of such an analysis as the initial conditions for a thermomechanical analyses. This is one of the main objectives of the present work.

Even for the limited aims of this work a variety of issues require consideration. Some of the main physical and numerical aspects of this problem may be listed as follows:

(a) A robust and efficient transient incompressible flow solver is required in order to model the metal flow into the mould. This solver must also be able to model a moving free surface,

CCC 0271–2091/95/060493–14

Received 10 March 1994
Revised 2 November 1994

hence a choice must be made between one of several formulations. The choice that is natural for moving boundary problems are Lagrangian and ALE (Arbitrary Lagrangian–Eulerian)[1–3] methods which allow the explicit determination of the free surface and have certain advantages in modelling advection-dominated transport. The main drawback of these methods is the requirement of a robust unstructured automatic mesh generator as frequent remeshing will be required due to the rapid distortion and movement of the free surface. For 3D problems especially, this is a serious limitation. Of the various Eulerian methods, one has to choose either between implicit methods, based on a mixed velocity–pressure formulation,[4] or semi-implicit segregated velocity pressure formulations.[5–7] Because of the advection-dominated nature of the problem, fully implicit methods are not suitable. In view of these facts the segregated approach has been chosen in this work.

(b) If an Eulerian approach is chosen, it is necessary to select a technique which is suitable for tracking the free surface on a fixed finite element mesh. The method used here is based upon the *Volume of Fluid* Method (VOF).[8] Using this technique, the moving metal front is represented by a nodal variable which is advected using the velocities from a solution of the Navier–Stokes equations. A laminar flow regime is assumed in this work, which implies that the thin boundary layer at the walls, where most of the velocity variation occurs, is not modelled. Thus, if the actual boundary condition of zero velocity at the walls is rigidly applied, this would lead to a very sluggish and unrealistic movement of the fluid at the wall. This problem is remedied by allowing the fluid to slip at the walls.[9]

(c) Once the velocities and the metal surface have been determined, the temperature field has to be calculated. It is clear that a very high temperature gradient exists in the vicinity of the metal surface which must be faithfully transported. The advection-dominated nature of the transport requires that special techniques are used, as it is well known that the conventional Galerkin Finite Element Method (GFEM) fails in this situation. There are several ways of dealing with this problem. The Streamline Upwind Petrov–Galerkin method (SUPG)[10] has been very successful for steady-state problems. Other methods include space–time FEM, split-operator methods, adaptive FEM and combinations of these. The Taylor–Galerkin method[11] is more suitable for transient problems as the diffusion-like terms which are the main characteristic of the upwind methods, arise naturally in this method, from considering higher-order Taylor series terms during the temporal discretization stage. This method can be seen as a particular form of the more general SUPG method and possesses the same capacity to deliver excellent stability and smoothness in the advected variable field with negligible false diffusion.[9] For convection-dominated problems the timestep size is restricted because of accuracy-requirements. The explicit nature of the discretized equations resulting from the Taylor–Galerkin method is particularly suitable in this context as the cost per timestep is minimized.

(d) At any given time the metal occupies only a part of the flow mesh, therefore a fictitious material is necessary to fill the remaining portion. For the heat transfer calculations the properties of air are used for this material. Also, properties of the fictitious material are selected in order to minimize the effect on the actual flow field and to avoid numerical instabilities.

(e) As the metal flows along the mould walls, it cools by losing heat to the mould. The contact between the mould and metal is, in general, not perfect, which again requires careful treatment. Special interface elements, of zero thickness, are used to control the heat transfer from metal to mould based on values of heat transfer coefficient, which may be known or estimated.

(f) In real castings there exist small gaps at the joints and split lines of steel moulds. Sand moulds have a porous structure in addition to the split lines. These spaces provide routes for the air to escape from the mould as the metal fills. No such spaces exist in a finite element mesh. This problem has been dealt with in this work by having a large number of exits distributed on the flow boundary at appropriate locations. This allows the entrapped air to escape. However, if a solidification model, coupled with velocity suppression in the solid region, is not implemented, the metal will also escape. The sudden imposition of zero velocity boundary conditions when the metal reaches the outlets is another approach, but this can easily cause instabilities due to the introduction of shocks into the system.

(g) Other physical phenomena which are important, but have not been considered in this work are solidification during filling, surface tension effects and gas absorption.

Most other researchers working on the modelling of the mould filling problem use finite difference methods, often in conjuction with the SOLA-VOF[8] method for tracking the fluid front.[12–17] Hartin[13] gives a comparison of implicit and explicit solution techniques for casting simulations. The finite difference approach of Swaminathan and Voller[18] draws an analogy between the filling of a computational cell and the evolution of latent heat, resulting in an enthalpy-type formulation suitable for both filling and solidification.

Finite element approaches include that of Waite and Samonds,[19] who solve the Navier–Stokes equations using a segregated velocity–pressure formulation, including a Darcy term in the momentum equations, to model the effect of solidification of the velocity field. They use the VOF approach, using an upwinded form of the advection equation, to provide the free surface information. Backer[20] uses an unmodified SOLA-VOF algorithm but includes a facility for modelling processes which use backpressure or vacuum. Zhang and Liu[21] use a simplified model based on potential theory in which the free surface is modelled by using VOF in conjunction with the Bernoulli equation

GOVERNING DIFFERENTIAL EQUATIONS AND BOUNDARY CONDITIONS

The conservation equations and appropriate boundary conditions used in the present model are as follows.

Conservation of mass.

$$\nabla \cdot \mathbf{v} = 0 \tag{1}$$

where $\mathbf{v}$ is the velocity vector.

Conservation of momentum. An expanded version of the stress divergence form is used,

$$\rho\left(\frac{\partial \mathbf{v}}{\partial t} + \mathbf{v}\cdot\nabla\mathbf{v}\right) = -\nabla P + \nabla\cdot\mu(\nabla\mathbf{v} + (\nabla\mathbf{v})^T) + \rho\mathbf{g} \tag{2}$$

in which P is the pressure, μ the dynamic viscosity, ρ the density and $\mathbf{g}$ is the gravitational acceleration.

The essential, or Dirichlet, boundary conditions for the Navier–Stokes equations are specified in terms of the velocities at the boundaries.

$$\mathbf{v} = \mathbf{w} \quad \text{on } \Gamma_1 \tag{3}$$

Pressure may not be specified at the boundary as it is an implicit variable in an incompressible flow[4] which propagates at infinite speed to deliver a solenoidal velocity field. The natural, or

Neumann, boundary conditions may be applied as normal and/or tangential traction forces,

$$f_n = -P + 2\mu \frac{\partial v_n}{\partial n} \quad \text{on } \Gamma_2 \tag{4}$$

$$f_\tau = \mu\left(\frac{\partial v_n}{\partial \tau} + \frac{\partial v_\tau}{\partial n}\right) \quad \text{on } \Gamma_2 \tag{5}$$

where n and τ are the unit normal and tangent vectors, respectively. Also, $\Gamma_1 \cup \Gamma_2 = \Gamma$, and $\Gamma_1 \cap \Gamma_2 = \phi$, where, ϕ is the null set.

Conservation of the metal front position. A pseudo-concentration function is used to track the free fluid surface. If this function is represented by $F(x, y, t)$ for a 2D flow, the first-order pure advection equation, which conserves the function $F(x, y, t)$, is written as

$$\frac{\partial F}{\partial t} + \mathbf{v} \cdot \nabla F = 0 \tag{6}$$

A particular value of the pseudo-concentration function, F_c is associated with the free fluid surface,[9] and it can be tracked in time by simply plotting the contour of F_c at each timestep. The value of $F(x, y, t) = 0{\cdot}0 = F_c$ is used to mark the free surface, while $F(x, y, t) > 0{\cdot}0$ indicates the fluid region and $F(x, y, t) < 0{\cdot}0$ the empty region. As this is a hyperbolic or pure advection equation, the boundary values of F are required only at the nodes where the fluid enters the cavity. A value of $F = 1{\cdot}0$ has been routinely used by the authors for this purpose.

Conservation of energy. Finally, the heat transfer is controlled by the advective–diffusive energy equation, which is

$$\rho c\left(\frac{\partial T}{\partial t} + \mathbf{v} \cdot \nabla T\right) = \nabla \cdot k \nabla T \tag{7}$$

where c and k are the specific heat and thermal conductivity, respectively, and T is the temperature.

Dirichlet boundary conditions for this equation consist of specified temperature values at the boundaries

$$T = \theta \quad \text{on } \Gamma_a \tag{8}$$

The general Neumann boundary condition for the energy equation may be written as

$$k \frac{\partial T}{\partial n} + q + h(T - T_a) = 0 \quad \text{on } \Gamma_b \tag{9}$$

where q, h and T_a are specified boundary heat flux, convective heat transfer coefficient and the ambient temperature, respectively. Γ_a and Γ_b must obey the same conditions as Γ_1 and Γ_2.

DESCRIPTION OF THE ALGORITHM

The Navier–Stokes equations are discretized using the fractional-step method of Donea *et al.*[5] The advection part of the Navier–Stokes equations is discretized via the Taylor–Galerkin procedure described by Laval and Quartapelle.[22] The Taylor–Galerkin procedure first suggested by Donea *et al.*,[11,23] has been used to discretize the pseudo-concentration equation and the energy equation. An unstructured mesh of four-noded quadrilateral elements has been used for

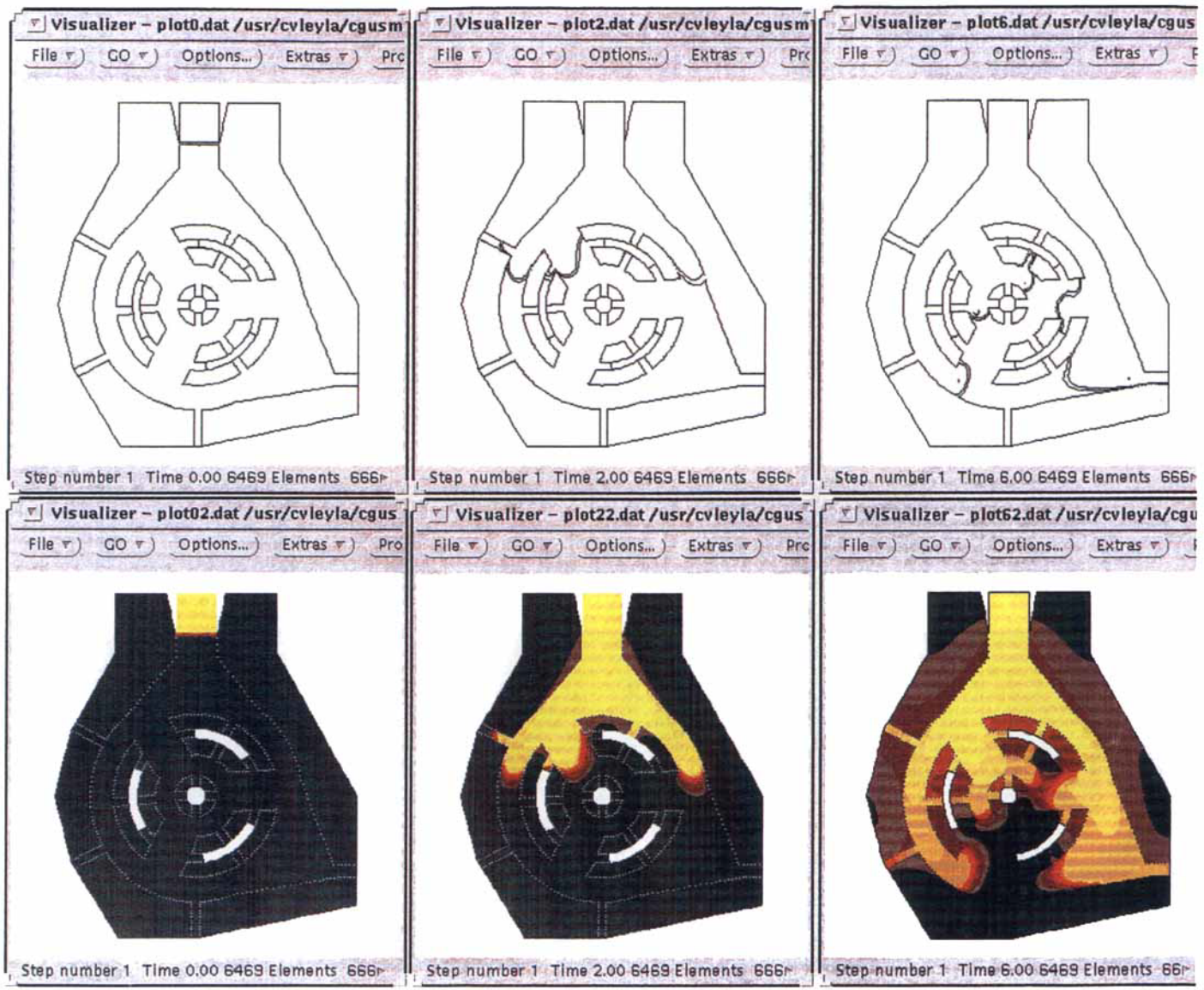

Plate 1. Front positions and temperature contours at 0.0, 2.0 and 6.0 seconds for the injection filling example (temperature range is from 700°C to 250°C)

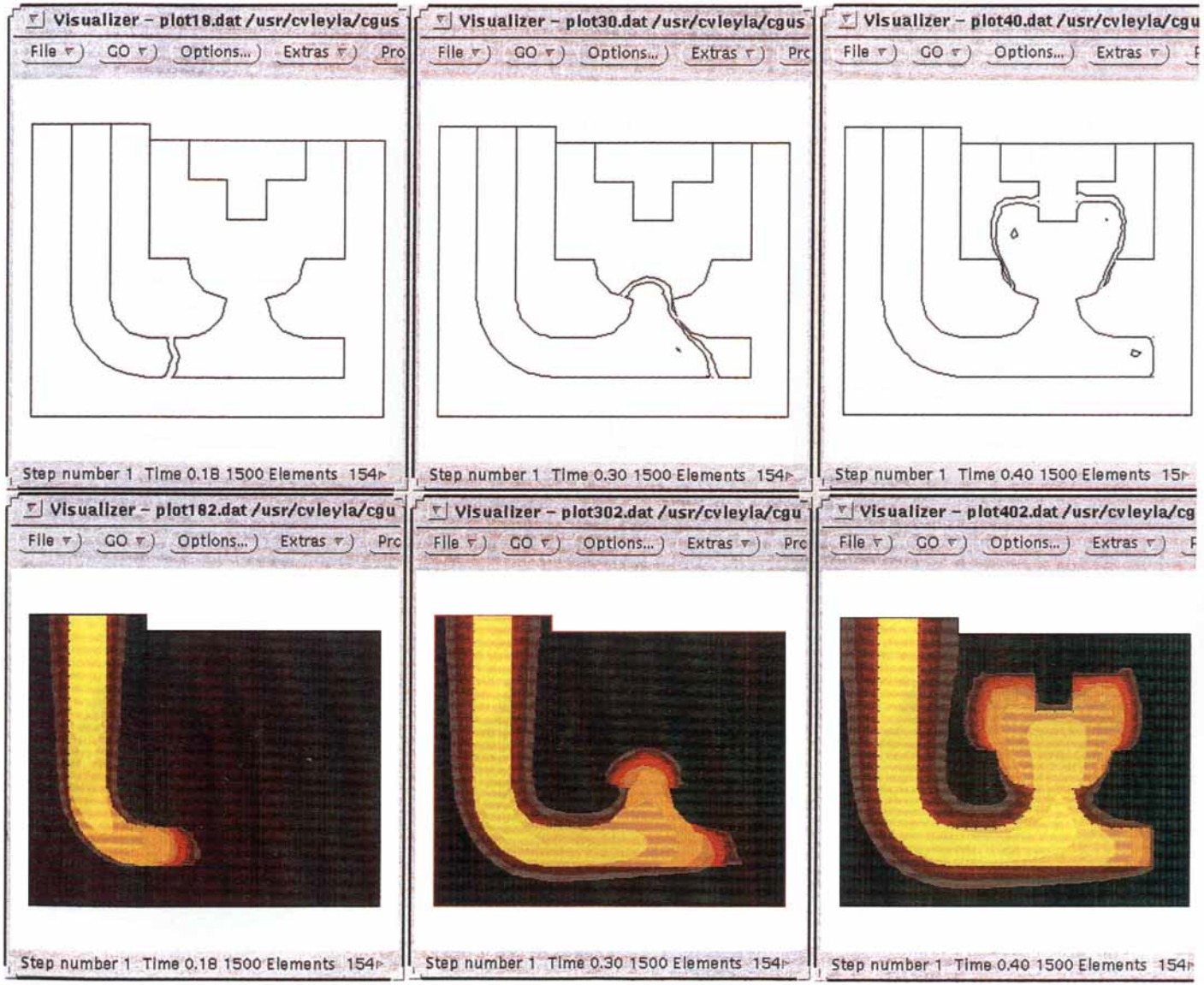

Plate 2. Front positions and temperature contours at 0.18, 0.3 and 0.4 seconds for the gravity filling example (temperature range is from 700°C to 300°C)

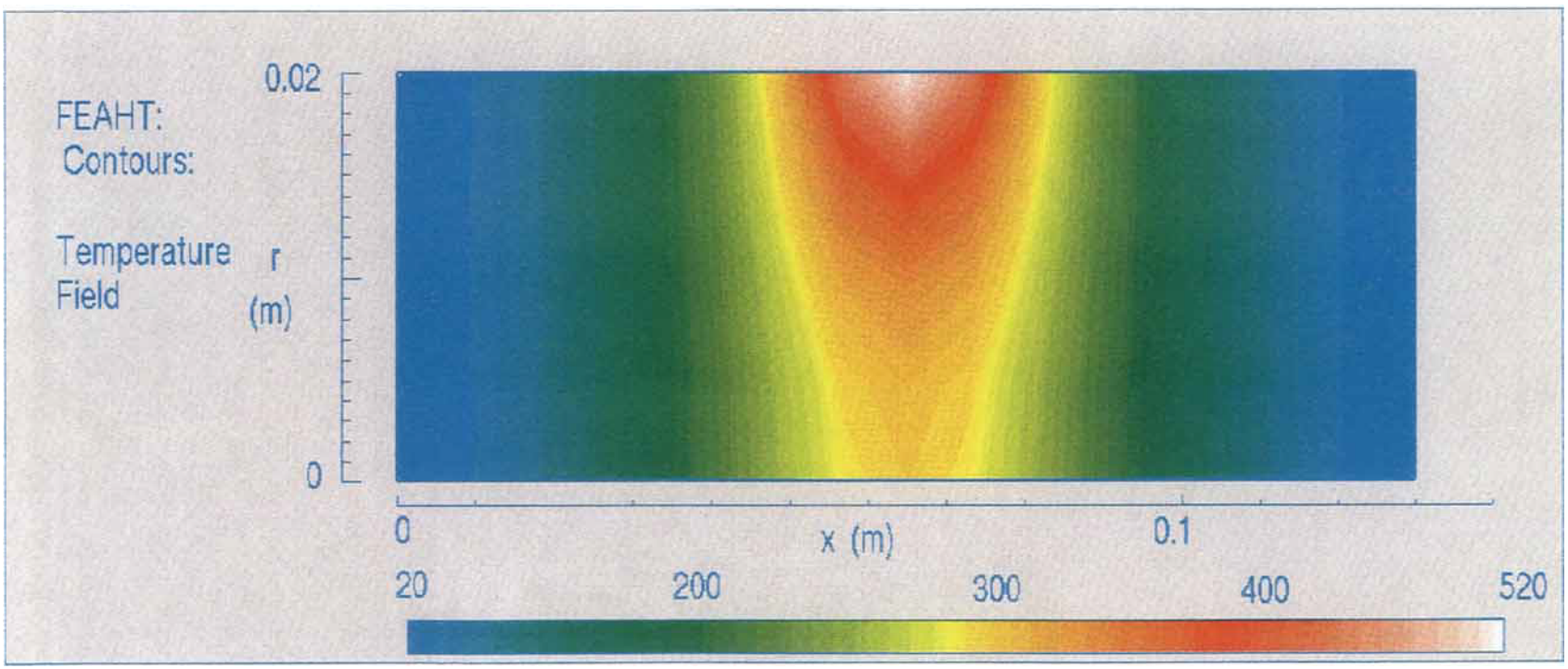

Plate 1. Temperature map of an aluminium alloy heated by induction at 8 kHz at the 12 s

the example problems. Linear shape functions have been employed for all the nodal variables except pressure which has been assumed to be constant over an element.

A detailed description of the full computational algorithm follows.

The flow field

The Navier–Stokes equations are solved in three separate stages: advection, viscous diffusion and incompressibility.

Advection

$$\frac{\partial \mathbf{v}}{\partial t} + \mathbf{v} \cdot \nabla \mathbf{v} = 0 \tag{10}$$

This equation is first discretized in time using the first two terms of the Taylor series expansion for the temporal derivative. The temporally discretized form obtained is

$$\frac{\mathbf{v}^* - \mathbf{v}_n}{\Delta t} = -(\mathbf{v}_n \cdot \nabla)\mathbf{v}_n + \frac{\Delta t}{2}(((\mathbf{v}_n \cdot \nabla)\mathbf{v}_n) \cdot \nabla)\mathbf{v}_n + \frac{\Delta t}{2}(\mathbf{v}_n \cdot \nabla)(\mathbf{v}_n \cdot \nabla)\mathbf{v}_n \tag{11}$$

where $\mathbf{v}^*$ is an intermediate velocity field, and $\mathbf{v}_n$ is the velocity at timestep n. This equation is now spatially discretized using the Galerkin form of the Finite Element Method (GFEM). The fully discretized system results in a matrix system of the form

$$\mathbf{M}_1 \left(\frac{\mathbf{v}^* - \mathbf{v}_n}{\Delta t} \right) = \mathbf{S}_1(\mathbf{v}_n) \tag{12}$$

As this equation represents the discrete version of the hyperbolic part of the Navier–Stokes equation, the only boundary conditions to be applied at this stages are the prescribed velocities flowing inward on Γ_1, or

$$\mathbf{v}^* = \mathbf{w} \quad \text{on } \Gamma_1 \,|_{\text{in flow}} \tag{13}$$

Equation (12) can now be solved explicitly if $\mathbf{M}_1$ is converted to a row-sum-type lumped mass matrix. However, a lumped mass approach will always degrade advection solutions.[24] Donea *et al.*[5] proposed an iterative explicit procedure which uses both lumped and consistent mass matrices to obtain a significantly improved solution.

Consider an equation system of the form

$$\mathbf{M}\mathbf{u} = \mathbf{f} \tag{14}$$

where

$$\mathbf{u} = \mathbf{u}_{n+1} - \mathbf{u}_n$$

(n being the time level). The iterative explicit procedure may be applied to this system according to the following relation:

$$\mathbf{L}\mathbf{u}^{p+1} = \mathbf{f} - (\mathbf{M} - \mathbf{L})\mathbf{u}^p \tag{15}$$

here $\mathbf{M}$ and $\mathbf{L}$ are consistent and lumped mass matrices respectively, and p is the iteration index. This procedure has been used here to obtain the intermediate step velocity $\mathbf{v}^*$ from equation (12). The matrix $\mathbf{S}_1$ in equation (12) is the advection matrix which includes terms arising from the Taylor–Galerkin discretization.

Viscous diffusion

$$\rho \frac{\partial \mathbf{v}}{\partial t} = \nabla \cdot \mu(\nabla \mathbf{v} + (\nabla \mathbf{v})^{\mathrm{T}}) + \rho \mathbf{g} \tag{16}$$

The equation is discretized by using a standard GFEM procedure to obtain

$$\mathbf{M}_2 \left(\frac{\mathbf{v}^{**} - \mathbf{v}^{*}}{\Delta t} \right) = \mathbf{K}_1(\mathbf{v}^{*}) + \mathbf{F}_1 \tag{17}$$

The prescribed velocity boundary conditions are applied as

$$\mathbf{v}^{**} = \mathbf{w} \quad \text{on } \Gamma_1 \tag{18}$$

and the viscous part of the natural boundary conditions are applied on boundary Γ_2. Equation (17) is solved explicitly using a lumped form of the matrix $\mathbf{M}_2$. An iterative solution is not necessary as the lumped explicit solutions for diffusion remain smooth is the timestep size is within specified stability limits. In equation (17), $\mathbf{K}_1$ is the standard viscous diffusion matrix and $\mathbf{F}_1$ is the force vector containing contributions from gravity and/or boundary loading.

Incompressibility. The velocity field obtained above ($\mathbf{v}^{**}$) does not, as yet, satisfy conservation of mass; the remaining equations to be dealt with are

$$\rho \frac{\partial \mathbf{v}}{\partial t} = -\nabla P \tag{19}$$

and

$$\nabla \cdot \mathbf{v} = 0 \tag{20}$$

If equations (19) and (20) are discretized via GFEM, we obtain

$$\mathbf{M}_3 \left(\frac{\mathbf{v}_{n+1} - \mathbf{v}^{**}}{\Delta t} \right) = \mathbf{C} P_{n+1} \tag{21}$$

$$\mathbf{C}^{\mathrm{T}}(\mathbf{v}_{n+1}) = 0 \tag{22}$$

where $\mathbf{C}$ is a gradient and $\mathbf{C}^{\mathrm{T}}$ a divergence matrix. Taking the divergence of both sides of equation (21) (after premultiplying by $\mathbf{M}_3^{-1}$) and cancelling the $\mathbf{v}_{n+1}$ term using equation (22), we have

$$\mathbf{C}^{\mathrm{T}} \mathbf{M}_3^{-1} \mathbf{C} P_{n+1} = -\frac{\mathbf{C}^{\mathrm{T}} \mathbf{v}^{**}}{\Delta t} \tag{23}$$

This equation is used to calculate the pressure, P_{n+1}. The final velocities may then be obtained from equation (21) and the forced boundary condition,

$$\mathbf{v}_{n+1} = \mathbf{w} \quad \text{on } \Gamma_1 \tag{24}$$

Further details and analysis of segregated velocity–pressure-type formulations for the finite element modelling of the incompressible Navier–Stokes equations may be obtained from Gresho.[6]

Pseudo-concentration function for front tracking

The pseudo-concentration equation (6) is a hyperbolic or pure advection equation. If the pseudo-concentration function is advected using conventional GFEM then severe oscillations are

usually generated. This problem can be remedied by a Taylor–Galerkin discretization of equation (6) as in Reference 9. If such a discretization is performed the following equation is obtained:

$$\frac{F_{n+1} - F_n}{\Delta t} = \left(-(\mathbf{v}_{n+1/2} \cdot \nabla) + \frac{\Delta t}{2} (\mathbf{v}_n \cdot \nabla)^2 \right) F_n \tag{25}$$

where $\mathbf{v}_{n+1/2}$ represents $(\mathbf{v}_{n+1} + \mathbf{v}_n)/2$. The fully discretized equations result in a matrix system of the form

$$\mathbf{M}_4 \left(\frac{F_{n+1} - F_n}{\Delta t} \right) = \mathbf{S}_2(F_n) \tag{26}$$

with the boundary condition,

$$F = 1{\cdot}0 \quad \text{on } \Gamma_1 |_{\text{in flow}} \tag{27}$$

This equation is solved using the iterative explicit procedure mentioned earlier. The advection matrix, $\mathbf{S}_2$, includes the diffusion-like terms arising from the Taylor–Galerkin discretization. An expanded form of this matrix may be found in Reference 9.

Heat transfer during filling

The heat transfer analysis of the filling process requires that both advection and diffusion are dealt with. To this end equation (7) is split into a convection and a thermal diffusion stage.

Convection

$$\frac{\partial T}{\partial t} + \mathbf{v} \cdot \nabla T = 0 \tag{28}$$

This equation is exactly the same as equation (6) for the pseudo-concentration function. A Taylor–Galerkin discretization of equation (28) results in an expression for an intermediate temperature field,

$$\frac{T^* - T_n}{\Delta t} = \left(-(\mathbf{v}_{n+1/2} \cdot \nabla) + \frac{\Delta t}{2} (\mathbf{v}_n \cdot \nabla)^2 \right) T_n \tag{29}$$

which is similar to equation (26). Spatial discretization of the above, using standard GFEM, results in a matrix system of the form

$$\mathbf{M}_5 \left(\frac{T^* - T_n}{\Delta t} \right) = \mathbf{S}_3(T_n) \tag{30}$$

subject to the boundary condition,

$$T = \boldsymbol{\theta} \quad \text{on } \Gamma_1 |_{\text{in flow}} \tag{31}$$

Again, this equation is solved using the iterative explicit procedure. The advection matrix, $\mathbf{S}_3$, includes the Taylor–Galerkin terms. An expanded form of this matrix may also be found in Reference 9.

Thermal diffusion

$$\rho c \frac{\partial T}{\partial t} = \nabla \cdot \nabla T \tag{32}$$

This part is discretized using standard GFEM and results in

$$\mathbf{M}_6\left(\frac{T_{n+1}-T^*}{\Delta t}\right)=\mathbf{K}_2(T^*)+\mathbf{Q} \tag{33}$$

with the fixed temperature boundary condition,

$$T=\theta \quad \text{on } \Gamma_a \tag{34}$$

The natural boundary conditions are included in the vector $\mathbf{Q}$ and $\mathbf{K}_2$ is the standard heat diffusion matrix. Temperatures at the end of the stage are calculated from equation (33) by the lumped explicit procedure.

STABILITY CONSIDERATIONS

Figure 1 shows the complete algorithm at a glance.

The explicit nature of this type of model means that timestep size limitations must be adhered to. This would normally make such a model more expensive than an implicit one. However, for advection-dominated flows, the timestep size is merely a reflection of the physics of the problem, and implicit algorithms, although stable with larger timesteps, require small timesteps to achieve acceptable accuracy. The actual timestep size limits are dictated by one of the following three criteria:

Thermal diffusion. For lumped explicit solution,

$$\Delta t \leqslant \frac{h^2}{\alpha}$$

where $\alpha = k/\rho c$.

Momentum diffusion. For lumped explicit solution,

$$\Delta t \leqslant \frac{h^2}{\nu}$$

Advection. For iterative explicit solution,

$$C \leqslant \frac{1}{\sqrt{3}}$$

where $C = v\Delta t/h$.

The mesh sizes are also limited due to the restriction of a maximum mesh Peclet number (Pe_g) for heat transfer and a maximum mesh Reynold's number (Re_g) for the flow. These limits are as follows.

Heat transfer:

$$(Pe)_g = \frac{vh}{\alpha} \leqslant 1$$

Momentum transfer:

$$(Re)_g = \frac{vh}{\nu} \leqslant 1$$

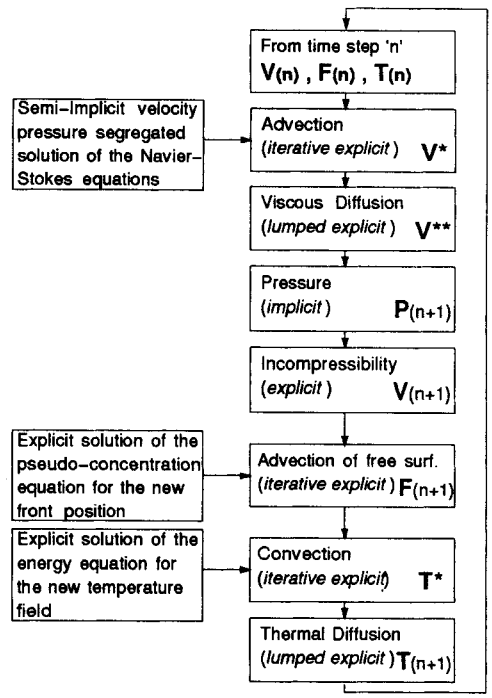

Figure 1. The filling simulation algorithm

The theoretical limit for these numbers is unity, however the solution remains stable for considerably larger values. The actual values of (Pe_g) and (Re_g) at which instabilities begin to appear depend upon the temperature or momentum gradients prevailing in the solution domain. For a low gradient the solution will remain stable for large value of (Pe_g) or (Re_g) and *vice versa*. For the examples presented in this paper, values for both (Pe_g) and (Re_g) of up to 25 were allowed without causing any instability.

METAL–MOULD INTERFACE ELEMENT

During the filling process (and during solidification after filling), thermal barriers exist at the metal/mould interface in the form of die coatings and/or air gaps. If the heat transfer at this

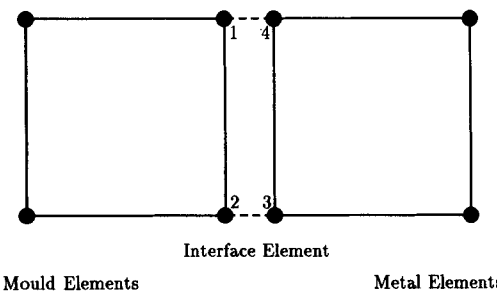

Figure 2. Interface element with its nodal connectivity

interface is to be accurately modelled, the heat transfer coefficient between the two faces must be known for all possible conditions. This information is not readily available. However, by incorporating interface elements,[25] whose stiffness depends upon the local heat transfer coefficient (suitable values of which must be estimated), a significant improvement can be achieved in the solution. Figure 2 shows a typical interface element. The stiffness matrix for the interface element is calculated by integrating over the length of the element only as its width is zero. This means that only one of the two sides of the interface element can be used to generate the whole matrix. The full stiffness matrix can be written as

$$\mathbf{K} = \left[\begin{array}{cc|cc} K_{11} & K_{12} & -K_{12} & -K_{11} \\ K_{21} & K_{22} & -K_{22} & -K_{21} \\ \hline -K_{21} & -K_{22} & K_{22} & K_{21} \\ -K_{11} & -K_{12} & K_{12} & K_{11} \end{array}\right] \tag{35}$$

from which it can be seen that all the terms in the matrix are obtained from the terms contained in the top-left quadrant, which can be calculated by

$$K_{ij} = \int_l h_f N_i N_j \, dl, \quad i = 1, 2 \text{ and } j = 1, 2 \tag{36}$$

where, l is the length of the interface element, h_f is the heat transfer coefficient and N_i and N_j are standard finite element shape functions. The stiffness contribution from the interface elements are incorporated in matrix $\mathbf{K}_2$ in equation (33) during the assembly process. In explicit calculations however, this is only symbolic as there is no need for assembly.

Test example of filling by injection

A realistic geometry shape is modelled to demonstrate a filling process representing pressure diecasting. The mesh for the cavity and the mould appears in Figure 3. The metal is injected into the mould with a uniform velocity from the inlet at the top (effect of gravity is not considered). The flow corresponds to an *Re* of 100·0. For the thermal analysis the real properties of metal (aluminium), air and die (steel) have been used.

$$\rho_{met} = 2700{\cdot}0 \text{ kg/m}^3 \quad k_{met} = 200{\cdot}0 \text{ W/mK} \quad c_{met} = 900{\cdot}0 \text{ J/kg K}$$
$$\rho_{air} = 1{\cdot}0 \text{ kg/m}^3, \quad k_{air} = 0{\cdot}025 \text{ W/mK}, \quad c_{air} = 1000{\cdot}0 \text{ J/kg K}$$
$$\rho_{die} = 7800{\cdot}0 \text{ kg/m}^3, \quad k_{die} = 48{\cdot}0 \text{ W/mK}, \quad c_{die} = 450{\cdot}0 \text{ J/kg K}$$

The coefficient of heat transfer for the metal–mould interface was assumed to be 30 000 W/Km^2. The mesh contained 6469 elements and 6662 nodes and was run for 10 000 timesteps. Three front positions and isotherms are shown in Plate 1.

It can be seen from the results of Plate 1 that the sharp thermal gradient at the metal front is maintained as the casting fills. The discontinuity of isotherms at the metal/mould interface is due to the interface elements. The front positions in Plate 1 are indicated by two constant value contour lines which enclose the contour value $F = 0{\cdot}0$. It can also be seen from the figure that the distance between these two lines remains practically unchanged throughout the analysis. This demonstrates that the pseudo-concentration function is also advected without any false diffusion. Also, it was not found necessary to smooth the pseudo-concentration field at any stage of the calculation.

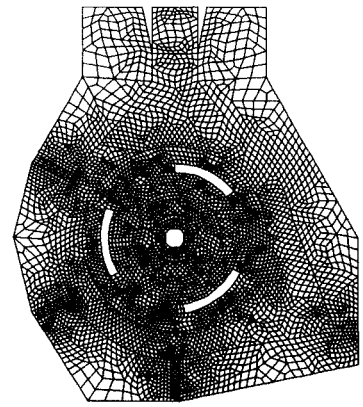

Figure 3. Mould and cavity mesh for the injection filling example

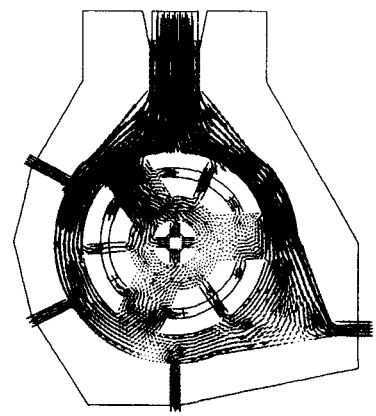

Figure 4. Velocity vectors for the injection filling example at 6·0 s

In order to properly fill the casting and provide adequate exits for the *air* to escape, 16 outlets were provided as seen from the velocity vector plot in Figure 4. This did allow the filling to proceed in a satisfactory manner, however, in the later stages of the filling more metal was *leaking* out of than filling the casting. A solidification model, implemented with a technique for velocity suppression in the solid region, needs to be developed to solve this problem. Furthermore, the same flow properties (density and viscosity) where used in both the *metal* and *air* regions to avoid constructing, factoring and solving the pressure matrix at every timestep. As the pressure solution is implicit, for this size of problem orders of magnitude more CPU time would be needed. More realistic filling patterns will be achieved if different properties for *metal* and *air* are used. As the timesteps used are very small due to stability requirements, the pressure solution changes very slowly, and subcycling[6] the pressure can be used to reduce the computing time.

Test example of filling by gravity

Another realistic problem was modelled to demonstrate filling in a gravity diecasting process. The mesh for the cavity and mould is shown in Figure 5. The metal enters the mould at the top

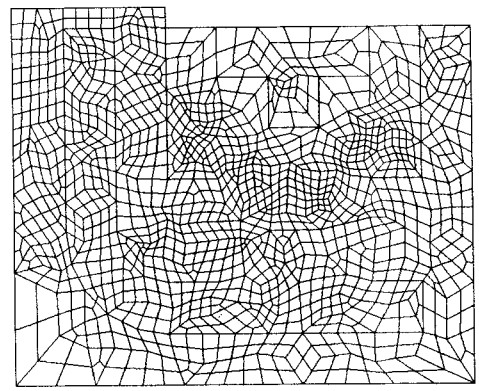

Figure 5. Mould and cavity mesh for the gravity filling example

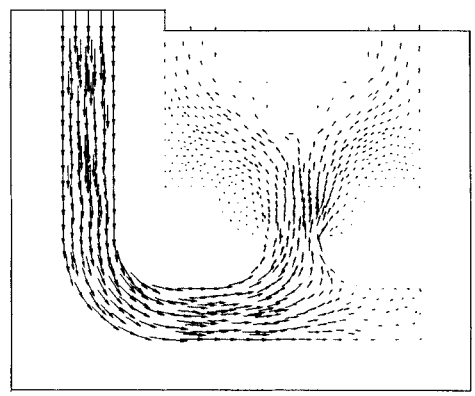

Figure 6. Velocity vectors for the gravity filling example at 0·4 s

left-hand side and accelerates as it fills down the sprue towards the casting. The flow corresponds to an *Re* of approximately 50. For the thermal analysis, the same properties as in the previous example were used. The heat transfer coefficient at the metal–mould interface for this example was assumed to be 10 000 W/Km^2.

The temperature and the front positions are shown in Plate 2. As demonstrated in the previous example, both the temperature and pseudo-concentration field are advected without excessive diffusion resulting in the preservation of the steep gradients. Identical flow properties for the *metal* and *air* were again used for this example. This results in unrealistic front positions as the metal fills the casting via the feeding system. However, there were no problems in filling the casting completely as there were only two exits, as seen from Figure 6.

CONCLUSIONS AND DISCUSSION

At this stage the model presented in this paper is only suitable for realistic thermal analysis. However, the main advantage is that it can provide practically useful results using computing

resources affordable by medium to small size industries. The temperature profiles from the two examples solved show little false diffusion and the interface elements produced realistic looking results as seen from the discontinuity of the temperature field at the metal-mould interface. These results are very encouraging in our quest for obtaining a high-quality initial thermal field from a mould filling analysis.

Further improvements can easily be made to enhance the utility of the model. The enthalpy method can be implemented to model solidification during filling. A combination of various convection modelling techniques, such as SUPG and adaptivity,[26] with the present scheme may further improve the resolution of the interface and also improve numerical stability. In general, finer meshes require smaller timesteps however, numerical instabilities are sometimes also caused by high gradients passing through coarse elements.

With the inherent advantages of the finite element method in terms of geometry resolution, it is expected that this model will provide an excellent foundation on which a realistic mould filling simulation facility may be built.

For a more realistic analysis of the filling process and free surface movement, far more sophisticated models are required which will need orders of magnitude more computing resources than available at present. Such models will probably be of a Lagrangian-type incorporating *state of the art* turbulence modelling techniques with fine resolution of the near wall regions.

REFERENCES

1. C. W. Hirt, A. A. Amsden and J. L. Cook, 'An arbitrary lagrangian-eulerian computing method for all flow speeds', *J. Comput. Phys.*, **14,** 227–253 (1974).
2. J. Donea, 'Arbitrary lagrangian-eulerian finite element methods', in *Computational methods for Transient Analysis,* Elsevier, Amsterdam, 1983, pp. 474–516.
3. B. Ramaswamy and M. Kawahara, 'Arbitrary Lagrangian-Eulerian finite element method for unsteady, convective, incompressible viscous free surface fluid flow, *Int. j. numer. methods fluids,* **7,** 1053–1075 (1987).
4. P. M. Gresho, R. L. Lee and R. L. Sani, 'On the time-dependent solution of the incompressible Navier–Stokes equations in two and three dimensions', in *Recent Advances in Numerical Methods in Fluids,* Vol. 1, Pineridge, Swansea, 1980.
5. J. Donea, S. Giuliani, H. Laval and L. Quartapelle, 'Finite element solution of the unsteady Navier–Stokes equations by a fractional step method', *Comput. Methods Appl. Mech. Eng.*, **30,** 53–73 (1982).
6. P. M. Gresho, 'On the theory of semi-implicit projection methods for viscous incompressible flow and its implementation via a finite element method that, also introduces a consistent mass matrix. Part 1: theory and Part 2: implementation', *Int. j. numer. methods fluids,* **11,** 587–659 (1990).
7. G. Comini, and S. DelGuidice, 'Finite element-solution of the incompressible Navier–Stokes equations', *Numer. Heat Transfer,* **5,** 463–478 (1982).
8. C. W. Hirt and B. D. Nichols, 'Volume of fluid (vof) method for the dynamics of free boundaries', *J. Comput. Phys.*, **39,** 201–225 (1981).
9. A. S. Usmani, J. T. Cross and R. W. Lewis, 'A finite element model for the simulation of mould filling in metal casting and the associated heat transfer', *Int. j. numer. methods eng.* **35,** 787–806 (1992).
10. A. N. Brooks and T. J. R. Hughes, 'Streamline upwind/Petrov–Galerkin formulations for convection dominated flows with particular emphasis on the incompressible Navier–Stokes equations', *Comput. Methods Appl. Mech. Eng.*, **32,** 199–259 (1982).
11. J. Donea, 'A Taylor–Galerkin method for convective transport problems', *Int. j. numer. methods eng.* **20,** 101–119 (1984).
12. I. Ohnaka, 'Modelling of fluid flow and solidification in castings', in T. S. Piwonka, V. Voller and L. Katgermann, (eds.), *Modelling of Casting, Welding and Advanced Solidification Processes VI,* Palm Coast, Florida, 21–26 March 1993, The Minerals, Metals and Materials Society, ISBN-0-87339-209-4, pp. 337–348.
13. J. R. Hartin, 'A comparison of implicit and explicit solution techniques and results in numerical casting simulations', in T. S. Piwonka, V. Voller and L. Katgermann, (eds.), *Modelling of Casting, Welding and Advanced Solidification Processes VI,* Palm Coast, Florida, 21–26 March 1993, The Minerals, Metals and Materials Society, ISBN-0-87339-209-4, pp. 373–380.
14. D. M. Lipinski, W. Schaefer and E. Flender, 'Numerical modelling of the filling sequence and solidification of castings, in T. S. Piwonka, V. Voller and L. Katgermann, (eds.), *Modelling of Casting, Welding and Advanced Solidification Processes VI,* Palm Coast, Florida, 21–26 March 1993, The Minerals, Metals and Materials Society, ISBN-0-87339-209-4, pp. 389–396.

15. H. J. Lin and H. L. Tsai, 'Numerical simulation of an integrated filling-solidification casting system', in T. S. Piwonka, V. Voller and L. Katgermann, (eds.), *Modelling of Casting, Welding and Advanced Solidification Processes VI*, Palm Coast, Florida, 21–26 March 1993, The Minerals, Metals and Materials Society, ISBN-0-87339-209-4, pp. 380–388.
16. G. Kreziak, P. Gilotte and R. Hamar, 'Modelling of fluid flow during mould filling', in T. S. Piwonka, V. Voller and L. Katgermann, (eds.), *Modelling of Casting, Welding and Advanced Solidification Processes VI*, Palm Coast, Florida, 21–26 March 1993, The Minerals, Metals and Materials Society, ISBN-0-87339-209-4, pp. 435–442.
17. M. R. Tadayon, J. A. Spittle and S. G. R. Brown, 'Fluid flow and heat transfer modelling of mould filling in casting processes', in R. W. Lewis, (ed.), *Numerical Methods in Thermal Problems VIII*, Swansea, U.K., 12–16 July 1993, ISBN-0-906674-80-8, pp. 309–317.
18. C. R. Swaminathan and V. Voller, 'Numerical modelling of filling and solidification in metal casting processes: a unified approach', in R. W. Lewis, (ed.), *Numerical Methods in Thermal Problems VIII*, Swansea, U.K., 12–16 July 1993, ISBN-0-906674-80-8, pp. 284–296.
19. D. M. Waite and M. T. Samonds, 'Finite element free surface modelling', in T. S. Piwonka, V. Voller and L. Katgermann, (eds.), *Modelling of Casting, Welding and Advanced Solidification Processes VI*, Palm Coast, Florida, 21–26 March 1993, The Minerals, Metals and Materials Society, ISBN-0-87339-209-4, pp. 357–364.
20. G. P. Backer, 'Finite element free surface flow analysis: a new tool for foundry engineers', in T. S. Piwonka, V. Voller and L. Katgermann, (eds.), *Modelling of Casting, Welding and Advanced Solidification Processes VI*, Palm Coast, Florida, 21–26 March 1993, The Minerals, Metals and Materials Society, ISBN-0-87339-209-4, pp. 405–412.
21. Y. F. Zhang and W. K. Liu, 'Casting filling simulations of thin-walled cavities with solidification', in T. S. Piwonka, V. Voller and L. Katgermann, (eds), *Modelling of Casting, Welding and Advanced Solidification Processes VI*, Palm Coast, Florida, 21–26 March 1993, The Minerals, Metals and Materials Society, ISBN-0-87339-209-4, pp. 413–420.
22. H. Laval and L. Quartapelle, 'A fractional-step Taylor–Galerkin method for unsteady in compressible flows', *Int. j. numer. methods fluids*, **11**, 501–513 (1990).
23. J. Donea, S. Giuliani, H. Laval and L. Quartapelle, 'Time-accurate solution of advection–diffusion problems by finite elements', *Comput. Methods Appl. Mech. Eng.*, **45**, 123–145 (1984).
24. P. M. Gresho, R. L. Lee and R. L. Sani, 'Advection–dominated flows with emphasis on the consequences of mass lumping', in *Finite Elements in Fluids*, Vol. 3, Wiley, New York, 1978.
25. A. S. Usmani, 'Finite element modelling of convective–diffusive heat transfer and phase transformation with reference to casting simulation', Ph.D. Thesis, University of Wales, Swansea, 1991.
26. H. C. Huang and A. S. Usmani, *Finite Element Method in Heat Transfer*, Springer Verlag, London (1994).